Cretaceous Research xxx (2015) 1–14

Contents lists available at ScienceDirect

Cretaceous Research

journal homepage: www.elsevier.com/locate/CretRes

Provenance constraints on the Tremp Formation paleogeography (southern Pyrenees): Ebro Massif *VS* Pyrenees sources

D. Gómez-Gras [a, *], M. Roigé [a, b], V. Fondevilla [b], O. Oms [b], S. Boya [b], E. Remacha [b]

[a] *Unitat de Petrologia i Geoquímica, Departament de Geologia, Facultat de Ciències, Universitat Autònoma de Barcelona, Edifici C, 08193 Bellaterra, Barcelona, Spain*
[b] *Unitat d'Estratigrafia, Departament de Geologia, Facultat de Ciències, Universitat Autònoma de Barcelona, Edifici C, 08193 Bellaterra, Barcelona, Spain*

A R T I C L E I N F O

Article history:
Received 30 April 2015
Received in revised form
7 September 2015
Accepted in revised form 8 September 2015
Available online xxx

Keywords:
Provenance
Sediment routing
Petrography
Southern Pyrenees
Maastrichtian
Foreland basin
Tremp Formation

A B S T R A C T

A detailed petrological study has been performed for the end-Cretaceous clastic deposits of the southern Pyrenees. Provenance results indicate that the Maastrichtian systems from both the Àger and the Vallcebre synclines show compositional features that mainly consist of a high proportion of single and polycrystalline quartz grains, feldspar and plutonic fragments. By contrast, the sandstone systems of the Tremp syncline exhibit minor contributions from igneous source areas and higher amounts of carbonatic components. These results reveal that the Tremp basin had a source area interpreted as situated to the North in the uplifting Pyrenees. The fact that this basin does not show a high plutonic source signal indicates that the Àger and the Vallcebre basins had been fed from a distinct source area located to the South, here interpreted as the Ebro Massif. Thus, the differences mentioned above might imply that the Montsec High acted as a barrier, avoiding a southern influence in the Tremp basin.

1. Introduction

Sand petrography is a powerful tool to investigate sediment provenance and to reconstruct paleogeographic basin evolution. The provenance of clastic deposits in foreland basins has been widely investigated because it provides valuable information about the erosional history of the fold-and-thrust belt that supplies the detrital material (e.g., Graham et al., 1986).

Sandstone petrography has been widely applied to the Eocene basins of the Pyrenean mountain belt, but few studies have been performed in the Maastrichtian part of the foreland basin (Tremp Formation, Mey, Nagtegaal, Roberti, & Hartelvelt, 1968). Although a detailed sedimentological and chronostratigraphic framework have been constructed for this end-Cretaceous marine-to-continental unit during the last decade, little is known about the nature and provenance of the clastic components that mainly feature the environments of the Tremp Formation. Most previous authors argued for an eastern origin (Sardinia Massifs) for the South Pyrenean sedimentary supply because of its East-West orientation (Ullastre & Masriera, 1982), and a possible influence of the southern Ebro Massif has never been documented.

The Ebro Massif was initially defined by Misch (1934) as the emerged zone mostly coincident with the present-day Ebro basin. This Massif was the southern boundary of the Cretaceous basins of the Pyrenean zone. Ashauer and Teichmüller (1935) described the Ebro Massif as a source area, mainly consisting of Paleozoic rocks, active from the Early Mesozoic until the Eocene. Llopis (1947), Rosell (1963), Combes (1969), Van Hoorn (1970) and Jurado (1988) among others, reported the role of the Ebro Massif as a contributing source area for the Pyrenean zone since at least the Early Cretaceous until the Paleogene when the Ebro basin developed. Although the occurrence of the Ebro Massif has been reported widely, it has not been characterised in terms of an active contributing source area. Despite this, all authors agree with the occurrence of the Ebro Massif, but our study is the first to explore it as a source area for the south Pyrenean zone in the Upper Cretaceous. This could have a strong implication for studies dating the Pyrenees exhumation on the basis of detrital zircons or apatites found in the south Pyrenean basins (Whitchurch et al., 2011). These studies associate its exhumation and provenance data to the tectonic evolution of a single source area in the Pyrenees without considering the existence of additional source areas that could

* Corresponding author.
E-mail address: David.Gomez@uab.cat (D. Gómez-Gras).

http://dx.doi.org/10.1016/j.cretres.2015.09.010
0195-6671/© 2015 Published by Elsevier Ltd.

supply these grains. Petrological studies are crucial to an accurate assignation of the exhumation signals to the distinct source areas that could provide sediment to a basin, to avoid misinterpretations of the exhumation history of thrust belts with complex source to sink patterns. This study provides new data on the provenance of the clastic systems during the early stages of the South Pyrenean foreland basin, contributing to the reconstruction of a more detailed paleogeographic evolution and a better characterisation of its sediment routing systems. The compositional features of the Tremp Formation are here used to determine the nature and location of the source areas of the Àger, Vallcebre and Tremp basins (Fig. 1). Sediment routing and evolution of source areas here contribute to a detailed understanding of paleogeographic changes within a relatively narrow time span. The vast knowledge of Pyrenean geology (a reference orogen for tectonosedimentary relationships) permits integration of our petrological data with structural, sedimentological and paleontological studies. This integration is intended to produce a detailed paleogeographic evolution for the framing a well-known continental record of the Maastrichtian in Eurasia. Paleogeographic reconstructions are necessary to expand on (Liebau, 1973; Oms et al., 2015) or improve previous ones (Plaziat, 1981; Rosell, Linares, & Llompart, 2001) or reinforce large scale reconstructions (Ziegler, 1990)

2. Geological and stratigraphic framework

The Pyrenees (Fig. 1) are a fold and thrust belt that developed foreland basins both on the southern and northern sides of the orogen (Muñoz, 1992). The South Pyrenean foreland basin was active from the Late Cretaceous until the Oligocene, had an East-West orientation and was connected to the Atlantic Ocean until the Late Eocene (Costa et al., 2010). During the Maastrichtian and Paleocene, this basin was partially filled with terrestrial strata known as the Tremp Formation (Mey et al., 1968). The Tremp Formation is found in several thrust sheets (Fig. 1): Bóixols-Sant Corneli, Montsec, Serres Marginals, Pedraforca and Cadí (Rosell et al., 2001). Cuevas (1992) and later Pujalte and Schmitz (2005) elevated this formation to the category of Group, dividing the former Tremp Formation into several minor formations according to internal stratigraphic differences. Hence, the Conques and Talarn Formation replaced the Maastrichtian portion of the Tremp Formation (or 'Lower Red Garumnian' *sensu* Rosell et al., 2001). The Paleocene strata of the Tremp Formation (or 'Upper Red Garumnian' of Rosell et al., 2001) were considered to include the Esplugafreda and Claret Formations. Here, we use the original name, the Tremp Formation, because of its applicability in all of the studied sectors, similar to the 'Garumnian' facies of Rosell et al. (2001).

The syntectonic nature of the Tremp Formation has been the goal of several studies (Ardévol, Klimowitz, Malagón, & Nagtegaal, 2000; Deramond, Souquet, Fondecave-Wallez, & Specht, 1993; Díaz-Molina, 1987; Eichenseer, 1988; Garrido-Mejias & Rios, 1972; Liebau, 1973; Simó & Puigdefabregas, 1985; Souquet, 1967). This syntectonic feature results from southwards thrust propagation of the Bóixols-Sant Corneli, Montsec, Serres Marginals, Pedraforca and Cadí thrusts (Fig. 1). These thrusts have a displacement of up to tens of kilometres and are reactivated from growth structure early faults that were active during the basin infill from the Late Cretaceous to the Eocene (Teixell & Muñoz, 2000). Synsedimentary folding and thrusting led to the partitioning of the Maastrichtian foreland into sub-basins (broken foreland basin). These sub-basins are known as the Tremp, the Àger and the Vallcebre and are synclines, in which the axes conform to belonging to basin depocentres (Fig. 1). Each basin was asymetrical, having its most active margin to the north. The Tremp basin was bounded to the north by the Bóixols Sant Corneli fold structure thrust and by the precursor of the Montsec thrust to the south (Deramond et al., 1993; Díaz-Molina, 1987). The Àger basin was bounded by the Montsec thrust structure to the north and by the Ebro Massif (passive margin) to the South (Teixell & Muñoz, 2000). The Serra del Cadí outcrops were in the southern part of the basin and underwent little thrusting (parautochtonous) in the southern boundary of the basin. The current location of the lower and upper Pedraforca thrusts results from their allochtonous character (Vergés & Martínez, 1988). Thus, the Tremp Formation of the lower and upper Pedraforca thrusts was originally northwards of the Cadí outcrops (basin depocentre).

The Tremp Formation, also known as 'Garumnian' (Leymerie, 1862), has been mostly studied for its reference geological and paleontological record. Stratigraphically, it can be subdivided into four units (Rosell et al., 2001): a marine-to-continental or lagoonal 'Grey Garumnian' (the Posa Formation of Cuevas, 1992) composed of greyish marls with invertebrate fauna, charophyte limestones and coals; a fluvial-deltaic 'Lower Red Garumnian', represented by reddish mudstones, sandstones and paleosols; a lacustrine unit with charophyte limestones and *Microcodium* known as 'Vallcebre limestones and laterally equivalent strata' (Rosell et al., 2001), and a fluvial 'Upper Red Garumnian' characterised by red mudstones, sandstones and conglomerates (Fig. 2). The former two units are Maastrichtian on the basis of the occurrence of dinosaurs, and because of rudist, charophyte and planktonic foraminiferan biostratigraphy and magnetostratigraphy (Díez-Canseco, Arz, Benito, Díaz-Molina, & Arenillas, 2014; Feist & Colombo, 1983; Galbrun, Feist, Colombo, Rocchia, & Tambareau, 1993; Oms et al., 2007; Riera, Oms, Gaete, & Galobart, 2009; Vicens, Ardèvol, López-Martínez, & Arribas, 2004; Vicente, Martín-Closas, Arz, & Oms, 2015; Vila et al., 2012). The 'Grey Garumnian' is similar to lagoonal settings in the Tremp and Vallcebre synclines from the Early Maastrichtian, but in the Àger syncline it is a more confined lacustrine environment (Villalba-Breva & Martín-Closas, 2012). In the Tremp syncline (Figs. 1 and 2), the 'Lower Red Garumnian' is mainly represented by fine-grained sandstone bodies that represent meandering rivers with tidal influence (Díez-Canseco et al., 2014). These sandstones are interbedded with thick mudstone units deposited in the floodplains. In the Vallcebre syncline (Figs. 1 and 3), the unit appears mainly as fine deposits and scarce sandstone bodies until the very end of the Maastrichtian. Then, coarse sandstone facies representing braided rivers (Reptile sandstone, Ullastre & Masriera, 1982) indicate a maximum regression peak (Oms et al., 2007). Finally, in the Àger syncline and the Benabarre sector (Figs. 1 and 3), the 'Lower Red Garumnian' records a transition from fine reddish mudstone deposits with isolated sandstone bodies to a thick, coarse sandstone units. This facies shift occurred at the beginning of the late Maastrichtian (Galbrun et al., 1993). After the K-Pg transition, there was a major change to the landscapes of the south Pyrenean basin. Hence, the former fluvial-deltaic 'Lower Red Garumnian' was replaced by lacustrine limestones during the Danian (López-Martínez, Arribas, Robador, Vicens, & Ardèvol, 2006) in the entire Pyrenean area.

Despite all of the investigations performed on the Tremp Formation, its petrology remains largely unknown. A provenance study of the Tremp Formation has potential for characterising paleogeographic evolution in terms of physical barriers (thrust-related faults) that controlled sediment routing during the early stages of a foreland basin.

3. Methods

3.1. Sandstone petrography

Sample localities were selected to obtain the most representative petrofacies of the Tremp Formation from the Àger, the

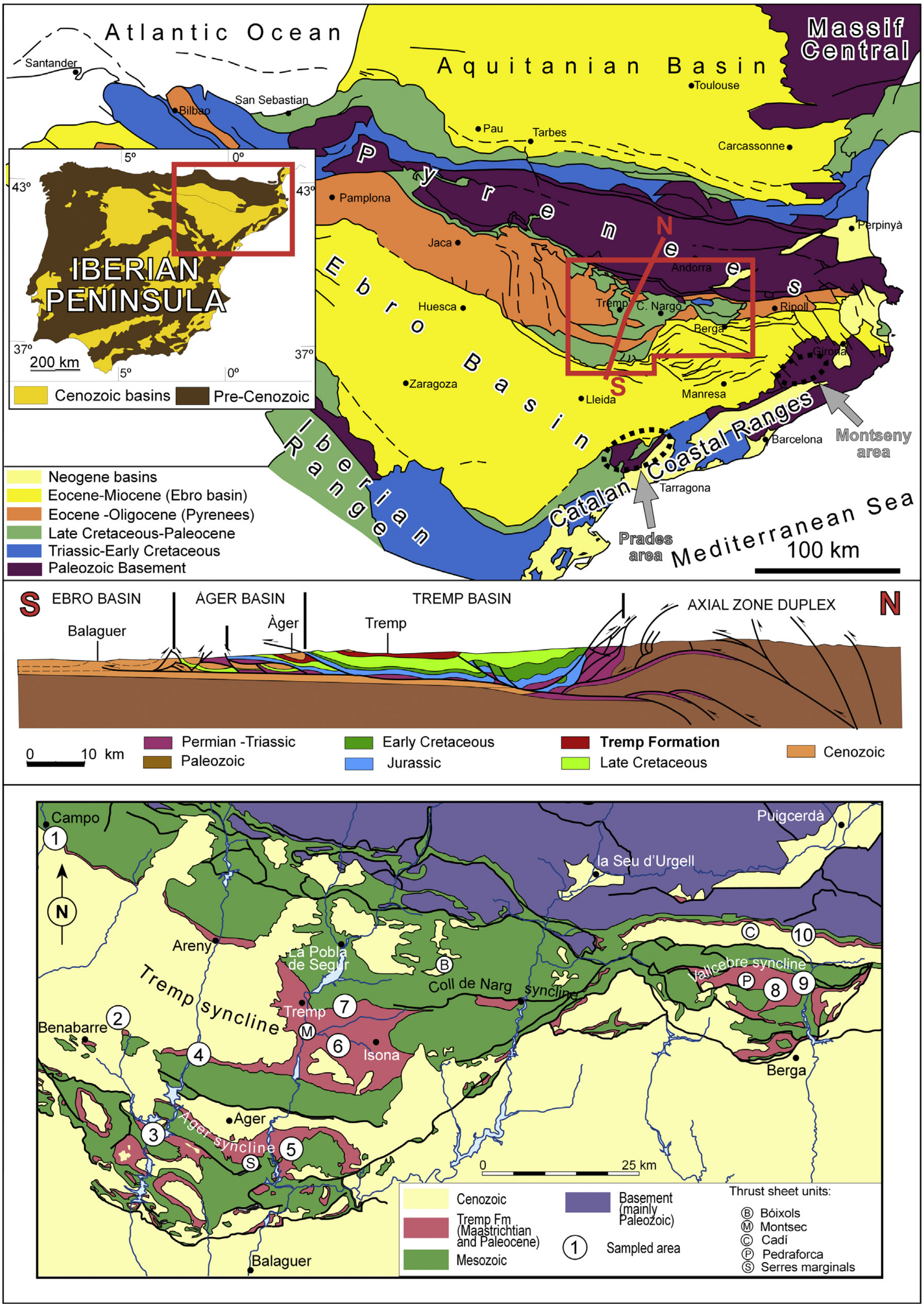

Fig. 1. Top: Geological setting of NW Iberia showing the Pyrenees, Catalan Coastal Ranges and Iberian Ranges. See location of the geological cross-section at the middle of the figure. Middle: reconstruction by Muñoz (1992) based on the ECORS profile. Bottom: Tremp Formation outcrops of the southern Pyrenees, with locations of the sampled sections. 1: Campo; 2: Benabarre/Benavarri; 3: Embassament Canelles; 4: Montrebei; 5: Fontllonga; 6: Costa de Castelltallat, Costa de la Serra and Masia de Ramon; 7: Orcau; 8: Mina Tumí; 9: Cal Borni-Mirador de Vallcebre; 10: Coll de Pal.

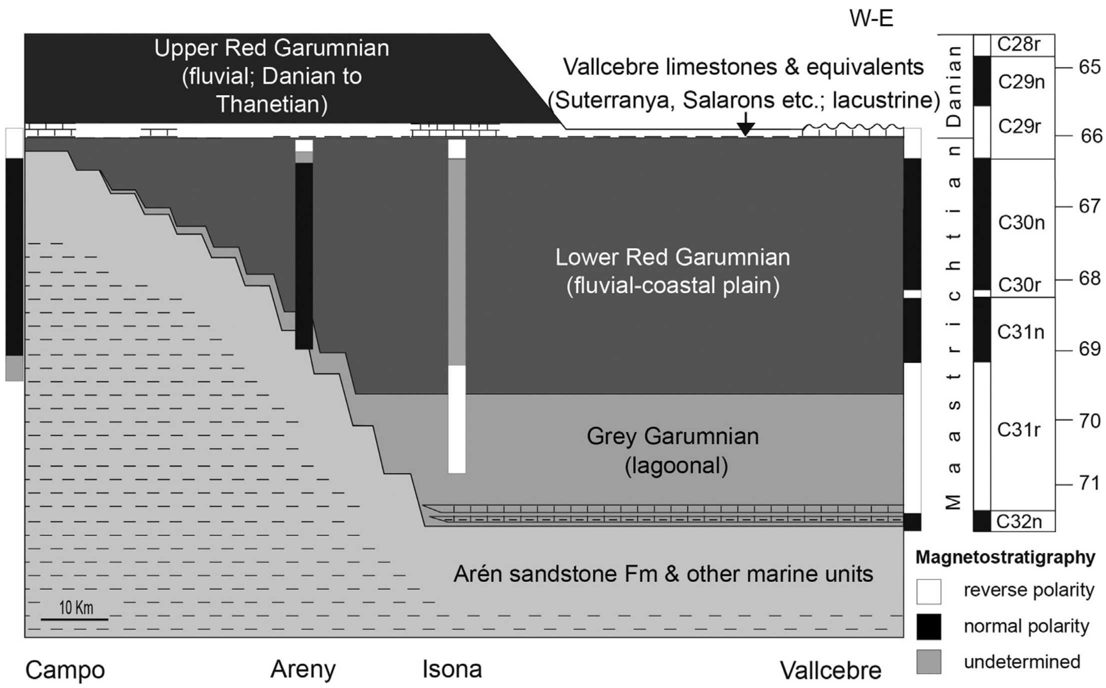

Fig. 2. Chronostratographic framework of the south Pyrenean Maastrichtian basin. Lithostratigraphic units after Rosell et al. (2001). Paleomagnetic data of Campo, Areny, Isona and Vallcebre after Canudo et al. (2015), Pereda-Suberbiola et al. (2009), Vila et al. (2012) and Oms et al. (2007), respectively. Standard Scale after Ogg and Hinnov (2012).

Vallcebre and the Tremp synclines. Samples from the Àger syncline and Benabarre sector were collected from the Fontllonga and the Benabarre sections (Fig. 3) where the 'Lower Red Garumnian' crops out, providing good quality samples. Samples from the Vallcebre syncline were obtained from the Vallcebre section (Fig. 3), and a complementary section was analised in the Coll de Pal sector (Cadí area). In the Tremp syncline, samples were collected from the sandstone bodies of the Orcau and the Montrebei sections (Fig. 3). A total of 51 sandstone samples were collected and examined in thin section under a polarizing microscope. From these samples, thirty-one were selected according to their representativeness and quality for a detailed petrographic study. Textural features, such as size and sorting were set for all of the samples following Beard and Weyl (1973). All thin sections were stained using Na-Cobaltinitrite (Chayes, 1952) for accurate identification of feldspar, and Alizarine red-S staining was applied for carbonates.

Quantification of detrital modes was performed by petrographic analysis of thin sections using the Gazzi-Dickinson point counting method (Dickinson, 1970; Gazzi, 1966; Zuffa, 1985). With this method, grain size effects are minimised, because it classifies crystals and other grains of sand size (>0.0625 mm) that occur in a larger rock fragment by the type of crystal below the cross-hair (Ingersoll et al., 1984) as well as the type of rock fragment. The point distance for counting was larger than the coarsest grain fraction in all studied samples (Van der Plas & Tobi, 1965). Three hundred to 500 points were counted for each thin section (according to Dryden, 1931), and 90 petrographic classes were considered, referring to framework grains (71 classes), matrix, cement and porosity (19 classes). Framework grains were grouped into the four main categories of Zuffa (1980): noncarbonate extrabasinal (NCE), noncarbonate intrabasinal (NCI), carbonate extrabasinal (CE) and carbonate intrabasinal (CI). All petrologic details of the samples can be found in the supplementary tables. Studied and illustrated material is deposited in the Departament de Geologia of the Universitat Autònoma de Barcelona (Petrology Unit). The reference code for each thin section/rock sample can be found in the Supplementary data.

3.2. Paleogeographic reconstructions

Paleogeographic studies of the south Pyrenean basin largely concern the Paleocene and later (Nijman, 1989; Puigdefàbregas, Muñoz, & Vergés, 1992; among so many others). For the Cretaceous, no accurate paleogeographic maps exist. The plots of Simó (1985) are the only available data, and they mainly focus on the marine successions of the Upper Cretaceous. Paleogeographic reconstructions shown here are not only based on petrology but also integrate other sources of information found in a myriad of studies indicated below.

A first major source of information is from tectonic reconstructions of thrust displacements. The current location of the Tremp Formation is the result of the Pyrenees shortening, a point not considered in previous reconstructions such as Plaziat (1981). Tectonic shortening forced the southward migration of cover units mainly during the Eocene (Muñoz, 1992). Displacements are calculated by considering the Ebro basin basement as the stable area. The displacement values are obtained by the unfolding of tectonically balanced sections by Vergés (1999), Vergés and Martínez (1988) and Vergés and Burbank (1996) for the western Pyrenees (Pedraforca and Cadí units), and Muñoz (1992) and Teixell and Muñoz (2000) for the south-central units (Bóixols-Sant Corneli, Montsec and Serres Marginals).

A second major source of information used to assist paleogeographic reconstructions is the subsurface information from oil exploration wells compiled by Lanaja (1987). These wells depict the distribution of the crystalline basement versus Triassic cover under the Ebro basin-Eocene rocks. This distribution constrains the extension of the exposed Paleozoic or Triassic source areas during the Late Cretaceous.

Other sources of information were obtained by reviewing studies concerned with paleocurent measurements, exhumation ages based on thermocronology (detrital zircons) and paleoenvironmental and sedimentological reconstructions.

Finally, paleogeographic schemes were plotted referring to the

Please cite this article in press as: Gómez-Gras, D., et al., Provenance constraints on the Tremp Formation paleogeography (southern Pyrenees): Ebro Massif *VS* Pyrenees sources, Cretaceous Research (2015), http://dx.doi.org/10.1016/j.cretres.2015.09.010

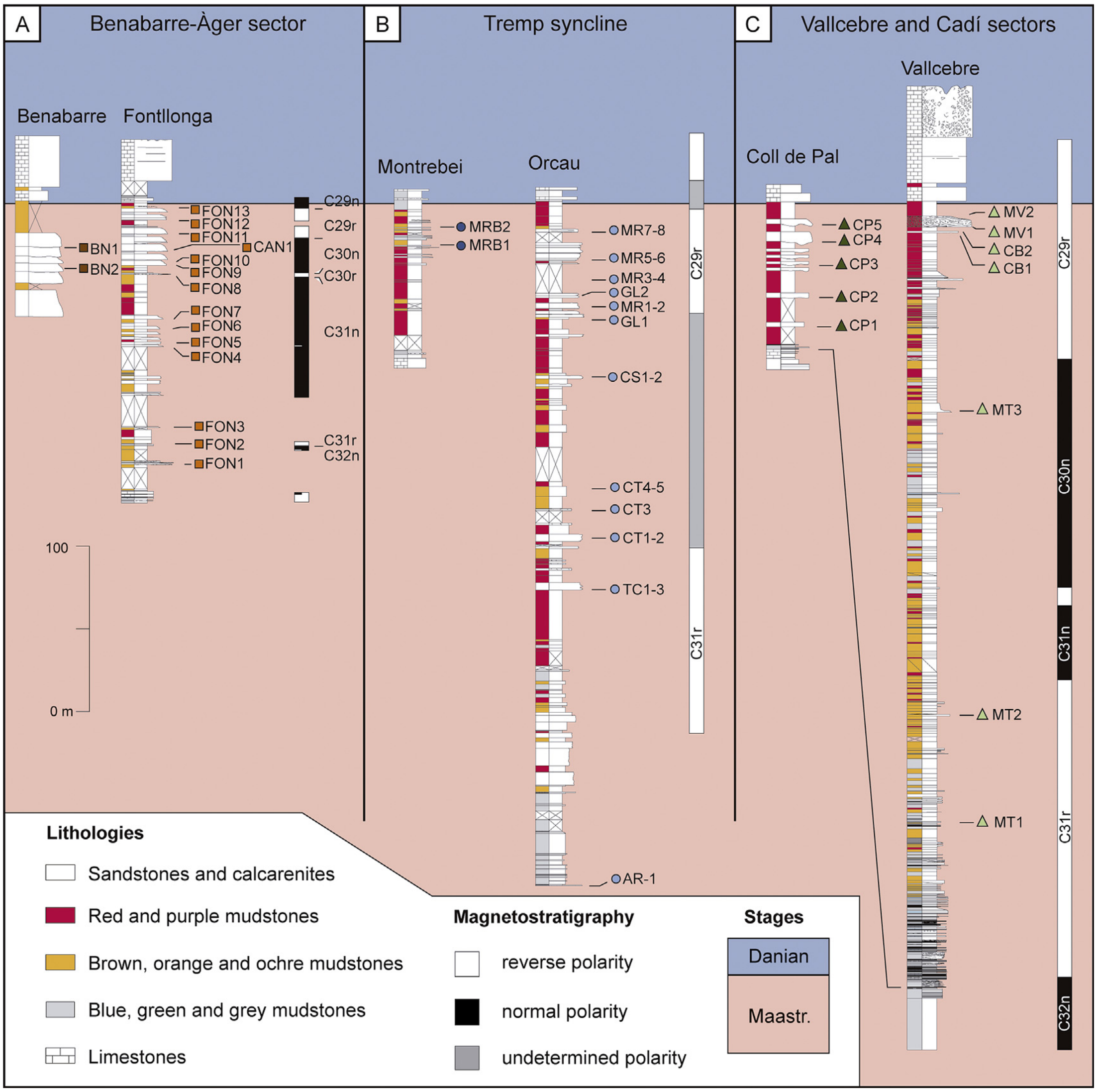

Fig. 3. Stratigraphic location of the studied samples. Paleomagnetic data after Galbrun et al. (1993), Oms et al. (2007) and Vila et al. (2012). (A) Samples from Benabarre (BN) and Fontllonga (FON) in their respective sections. Both sections can be directly correlated with each other (López-Martínez, Ardèvol, Arribas, Civis, & Gonzalez-Delgado, 1998). The sample from Embassament de Canelles (CAN1) is projected in the Fontllonga section. (B) Samples from Montrebei (MRB) and Orcau (TC and GL), Costa de Castelltallat (CT), Costa de la Serra (CS) and Masia de Ramon (MR). The latter are projected in a section measured in the Orcau area (modified from Oms et al., 2014). (C) Samples from Mina Tumí (MT), Cal Borni (CB) and Mirador de Vallcebre (MR) projected in a Vallcebre composite section.

current geographic border between Spain, France and Andorra. See Institut Geològic de Catalunya (2010) for additional data related to palinspastic reconstructions. The accurate geo-biochronological correlations and paleoenvironmental knowledge of the Tremp Formation has permitted the construction of four paleogeographic plots scattered within a time span of 5 Myr. These four plots belong to the (1), early Maastrichtian (2), Transition early-late Maastrichtian, (3) end Maastrichtian and (4) Paleocene. For the Àger basin, we mainly used data from Galbrun et al. (1993) and Villalba-Breva and Martín-Closas (2012), and for the Tremp basin, we used data from Vila et al. (2013), Pereda-Suberbiola et al. (2009) and Canudo et al. (2015). Finally, for the western Pyrenees (Vallcebre basin) we used data from Oms et al. (2007) and Vicente et al. (2015).

4. Results

4.1. Grain types

All samples show a structure supported by grains, where the matrix ratio is low (usually less than 10%). The main textural features are variable, mainly because of the grain size effect or because they are linked to the depositional environment. Most of the samples are poorly to moderately sorted with subangular to well-rounded grains.

4.1.1. Non-carbonate extrabasinal grains (NCE)

Grains classified as "Non-carbonate extrabasinal" are siliciclastic components, such as quartz, feldspar or lithic fragments. Quartz is a common component (Fig. 4A) that appears in all of the samples, with proportions ranging from 7% to 60% (described percentages for detrital grains are always referred in the total framework grains). The quartz has been classified as monocrystalline, coarse polycrystalline (crystals >0.0625 mm), fine polycrystalline (crystals <0.0625 mm) or contained in a rock fragment (sandstone, hybrid sandstone, metamorphic and plutonic rock) according to the Gazzi-Dickinson point counting method. Quartz with evaporitic inclusions (Fig. 4A) occurs in almost all of the samples but always in proportions less than 4%. Occasionally, quartz with inherited

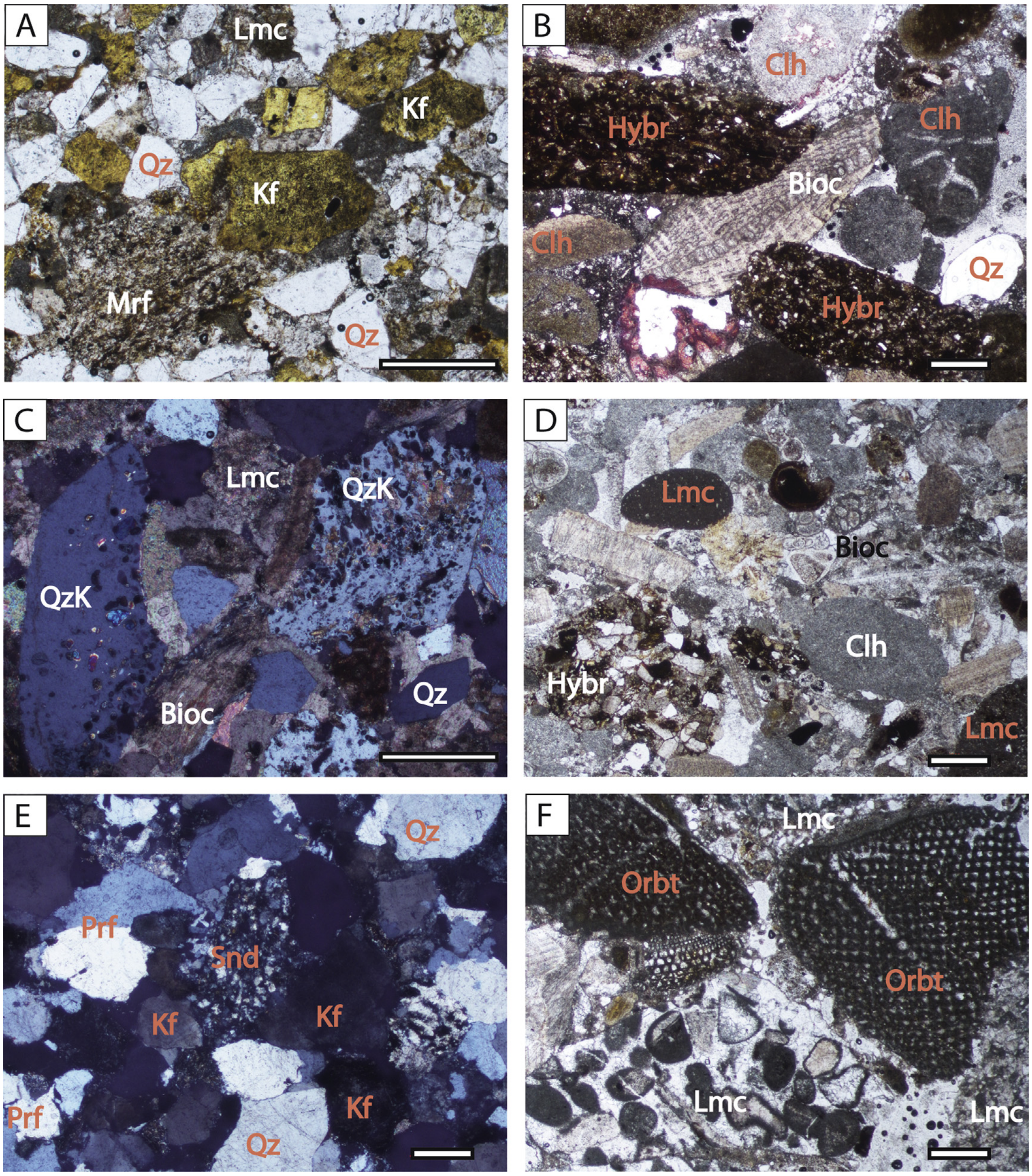

Fig. 4. Optical photomicrographs of extra and intrabasinal grains: (A) General view of "Mixed siliciclastic and carbonatic extrabasinal" petrofacies showing extrabasinal grains as quartz (Qz), K-feldspar (Kf), a schist metamorphic rock fragment (Mrf) and micritic limestones (Lmc) (plane polarized, PPL); (B) "Carbonatic extrabasinal enriched" petrofacies showing extrabasinal grains as hybrid sandstone rock fragments (Hybr), and carbonate intrabasinal grains as caliche nodules (Clh) and single foraminifera bioclast (Bioc) (PPL); (C) "Mixed siliciclastic and carbonatic extrabasinal" petrofacies showing some quartz grains riddled with salt crystal inclusions (QzK), bivalve fragments (Bioc) and sparitic limestone rock fragments (Lmc) (cross-polarized, XPL); (D) "Carbonatic extrabasinal enriched" petrofacies showing intrabasinal grains, such as foraminifera bioclasts (Bioc) and extrabasinal components, hybrid sandstone fragments (Hybr) and micritic limestone (Lmc) rock fragments (PPL); (E) "Siliciclastic dominant" petrofacies showing monocrystalline and polycrystalline quartz (Qz), orthoclase (Kf), plutonic fragments (Prf) and quartzarenite fragments (Snd) (XPL); (F) "Carbonatic extrabasinal enriched" petrofacies showing extrabasinal orbitolinid grains (Orbt) and grainstone and packstone rock fragments (Lmc) (PPL). The red scale bar is 1 mm. (For interpretation of the references to colour in this figure legend, the reader is referred to the web version of this article.)

syntaxial cement has been identified. Single-grain feldspar occurs in proportions lower than 20%. Feldspar (Fig. 4A, E) distinction has been made between orthoclase (<20%), microcline (0%) and plagioclase (<1%). K-feldspar appears fresh or, in some cases, slightly altered, whereas plagioclase grains show strong sericite alteration. Most of the samples have abundant lithic grains, classified as metamorphic (MRF), sedimentary (SRF) and plutonic (PRF) rock fragments. Metamorphic rock fragments (Fig. 4A) have been classified according to their composition and metamorphic rank (Garzanti & Vezzoli, 2003). The main types of metamorphic rocks that can be identified are very low to low-grade (metapelites and phyllites) and medium-grade (mica schists and schists). Non-carbonate sedimentary fragments are represented by sandstone, siltstone (Fig. 4B), chert and radiolarite rock fragments. Mixed carbonatic and siliciclastic sandstone fragments are also represented and are classified as hybrid siltstone or hybrid sandstone because of their content in intrabasinal and extrabasinal carbonatic components.

Muscovite and biotite are the most common phyllosilicatic grains (<1%), in some cases appearing as rock forming fragments, such as schists or granitoids. Heavy minerals are always less than 1%, and mainly are tourmaline and zircon, usually rounded to subangular.

4.1.2. Carbonate extrabasinal grains (CE)

Carbonate grains are widely represented in most of the samples, and are even dominant in some samples. Distinguishing between intrabasinal and extrabasinal carbonate grain was performed following Zuffa (1980, 1985). The proportion of extrabasinal carbonate grains (Fig. 4D) can be as high as 70%. Fragments of bioclastic limestones (Fig. 4F) have been classified according to Dunham (1962), appearing as micritic and bioclastic mudstone (<20%), packstone-wackestone (<18%) and grainstone (<14%). Cretaceous bioclasts can be identified in some of these fossiliferous limestones. Sparitic limestone fragments are also present and appear as monocrystalline calcite or as polycrystalline sparitic calcite fragments. Dolostone and dolomitized fragments are absent in all of the samples. Larger foraminifera identified as orbitolinids (Fig. 4F) imply an extrabasinal origin according to their Early Cretaceous age, and hence have been classified as carbonatic extrabasinal grains.

4.1.3. Carbonate intrabasinal grains (CI)

Carbonate intrabasinal grains comprise bioclasts (Fig. 4B, D), micritic coated grains, caliche nodules (Fig. 4B) and other micritic intraclasts (<30%). Bioclasts have been grouped into (i) larger benthic foraminifera and planktonic foraminifera (up to 7.5%), (ii) other bioclasts, mainly red and green algae, molluscs, ostracodes, bryozoans and corals (<15%), (iii) *Microcodium* grains (<5%) and (iv) silicified bioclasts (<1%). Micritic coated grains are oncolites and are usually nucleated around siliciclastic grains. Caliche nodules and micritic intraclasts can reach high proportions in some layers (up to 25%).

4.1.4. Non-carbonate intrabasinal grains (NCI)

Non-carbonate intrabasinal grains always appear in minor proportions and are represented by glauconite and argillaceous rip-up-clasts.

4.2. Diagenetic features

Authigenic minerals represent percentages ranging from 3% to 40% of the entire sample and are mainly related to cementation, which constitutes the main diagenetic process affecting sandstones of the Tremp Formation. Two component types have been classified: (i) calcite and ferroan calcite cement and (ii) ankerite cement. Pore-filling cement reaches amounts of up to the 25%, whereas cement replacing grains appear in lower percentages (<15%). Calcite is the most common authigenic mineral, occurring in intergranular primary porosity as well as intragranular in bioclasts and filling microfractures (secondary porosity). Calcite cement appears to replace some framework grains, such as quartz, K-feldspar, plutonic rock fragments, silicified limestone and sandstone fragments. Iron-free calcite is the main composition of pore-filling cement, whereas ferroan calcite appears mainly in the primary intragranular porosity of bioclasts and filling microfractures.

4.3. Petrofacies

The term petrofacies is used to describe clastic rocks with distinctive compositional features that can be clearly identified by the ratio of diferent grain types (Mansfield, 1971). Thus, analyses of lateral and vertical compositional variations of the Tremp Formation clastic sedimentary rocks allowed three main petrofacies to be recognised from the depocentres:

4.3.1. Carbonatic extrabasinal enriched petrofacies

The “Carbonatic extrabasinal enriched” petrofacies (Fig. 4B, D, F) can be distinguished by its dominant content of the following grain types (>50% from the total framework grains). Carbonatic extrabasinal grains are mainly represented by limestone rock fragments and monocrystalline and polycrystalline calcite grains. Intrabasinal grains (mainly bioclasts and micritic coated grains) always occur in percentages ranging from 5% to 30% of the total framework grains. This petrofacies can also be recognised by its low or absent feldspar content (K-feldspar and plagioclase) and by the particular dominance of sedimentary rock fragments over metamorphic and plutonic fragments.

4.3.2. Mixed siliciclastic and carbonatic extrabasinal petrofacies

Siliciclastic grains occur in proportions above the 50%, whereas carbonatic extrabasinal grains are between 10% and 40% of the total framework grains. Intrabasinal grains appear in proportions ranging from 1% to 20% and are mainly represented by micritic coated grains with lower contributions of bioclastic components. One of the most remarkable features of this group is the abundant content of K-feldspar (Plagioclase/K-feldspar < 1) and plutonic rock fragments. This contrasts strongly with the absence of these components in the “Carbonatic extrabasinal enriched” petrofacies described above. Metamorphic and sedimentary rock fragments are also common components that widely appear in all the samples of this petrofacies in variable proportions.

4.3.3. Siliciclastic dominant petrofacies

This petrofacies is highlighted by low extrabasinal and intrabasinal carbonatic grains content, that always appears in proportions less than 10% or is absent in most of the samples (Fig. 4E). Feldspar widely occurs as orthoclase with minor contributions of highly altered plagioclase, with the Plagioclase/K-feldspar ratio < 1. This group is also characterised by the high content of quartz grains (monocrystalline and polycrystalline) and plutonic rock fragments. Metamorphic and sedimentary grains are subordinate lithic grains, mainly represented by quartzarenite fragments, metamorphic quartzites and other low-medium grade metamorphic grains such as schists and shales.

4.4. Modal sandstone composition

Ternary diagrams (Fig. 5) have been used to classify and identify the main compositional changes for the studied systems. The modal composition of sandstones is represented here according to Zuffa (1980) (NCE-CE-CI); Dickinson et al. (1983) (QFL) and Gazzi, Zuffa, Gandolfi, and Paganelli (1973) (QFL+CE). Other diagrams have been used to analyse the lithic fraction, such as MRF-(PRF+F)-SRF (Fig. 5D). A first-order compositional classification has been obtained for all of the studied samples by representing the relative content of “non-carbonate extrabasinal” (NCE), “carbonate extrabasinal” (CE) and “carbonate intrabasinal” (CI) components.

4.4.1. Àger syncline and Benabarre sector

All samples from the Àger and the Benabarre sectors (Fig. 3) show higher proportions of non-carbonate components than carbonate components, with all of them plotted in the “sandstone” field sensu Zuffa (1980) (Fig. 5A), with a mean $NCE_{62}CE_{25}CI_{13}$. Concerning the quartz/feldspar/lithics content, the mean for this system is $Q_{67}F_{19}L_{14}$ (Fig. 5B), so samples can be classified as “subarkoses” (Pettijohn, Potter, & Siever, 1972). Single and polycrystalline quartz grains are common, some of them with evaporitic inclusions. Non altered K-feldspar appears as orthoclase (microcline is absent), with the plagioclase to K-feldspar ratio (P/K) less

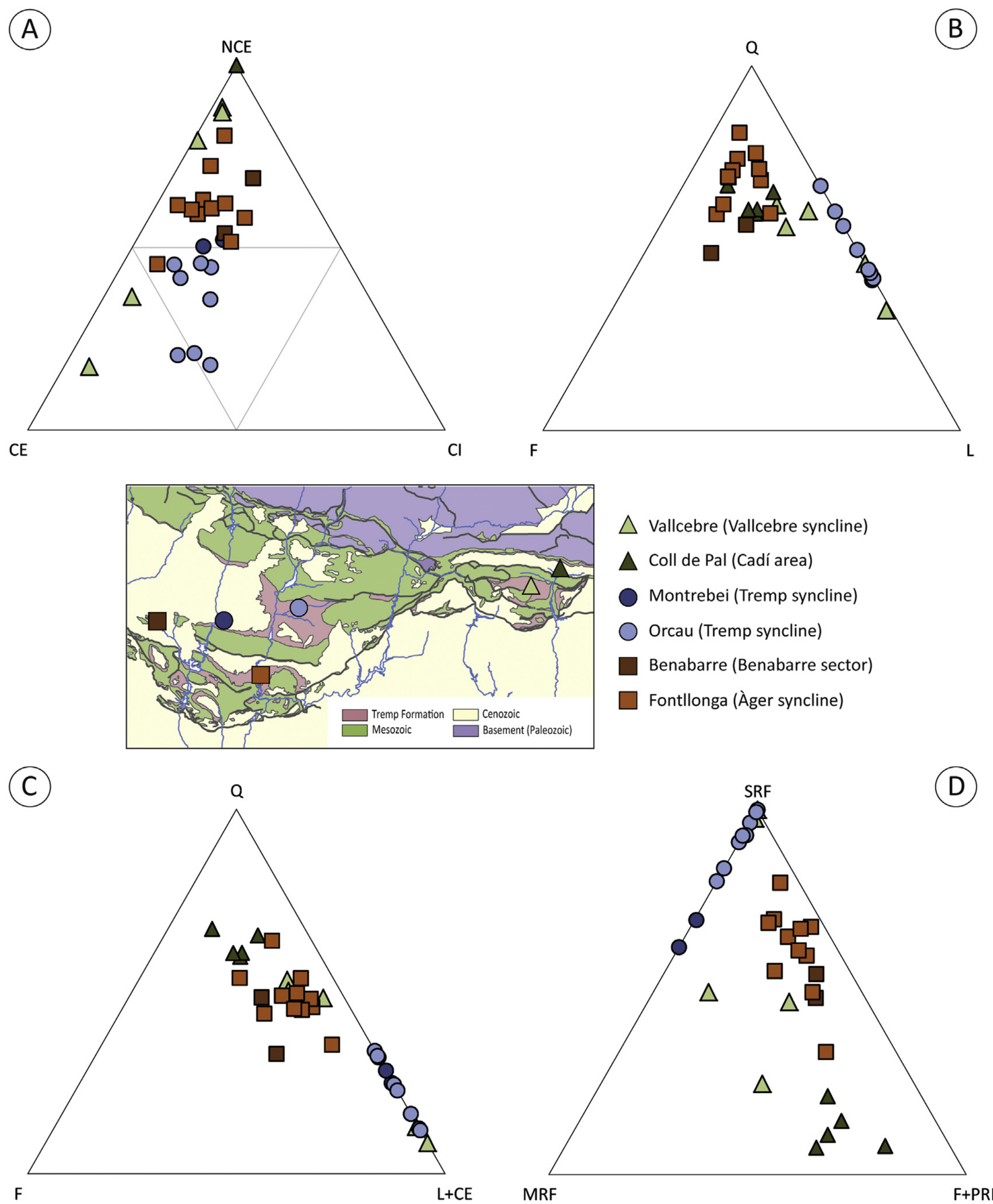

Fig. 5. Sandstone composition plots for the clastic systems of the Tremp Formation (see location in Fig. 2). Compositional ternary diagrams are: (A) First-order compositional plot (Zuffa, 1980) in which NCE, Non-Carbonate Extrabasinal grains; CE, Carbonate Extrabasinal; and CI, Carbonate Intrabasinal, (B) QFL compositional plot (Dickinson et al., 1983) in which Q, Quartz; F, Feldspar; and L, Lithic grains, (C) QFL + CE compositional plot (Gazzi et al., 1973) in which Q, Quartz; F, Feldspar; and L + CE, Lithic and carbonate extrabasinal grains, (D) Compositional plot of lithic grains in which SRF, Sedimentary rock fragments; MRF, Metamorphic fragments, and F + PRF, Feldspar and Plutonic fragments.

than 1. Most common carbonate extrabasinal grains are micritic and wackestone-grainstone grains, some of them with fossil content of miliolids and tintinnids. Intrabasinal components are coated grains, which occur in almost all samples, with a lower proportion caliche nodules, bioclasts (including carophytes) and *Microcodium* grains. No clear vertical trends can be observed along both the Fontllonga and the Benabarre sections. According to the compositional features, all of the samples from the Àger syncline correspond to "Mixed siliciclastic and carbonatic extrabasinal" petrofacies and can be easily distinguished in the different ternary diagrams (Fig. 5).

4.4.2. *Tremp syncline*

Samples from the Tremp syncline show a clear dominance of extrabasinal and intrabasinal carbonate grains over siliciclastic grains. Limestone fragments are grainstone, wackestone-packstone and biomicritic mudstone, similar to those described in the Àger syncline. Intrabasinal grain types are also similar, but bioclasts are much more abundant than coated grains and *Microcodium*. Some layers are rich in caliche nodules because of the reworking of interstratified calcrete soils. The mean for this sector is NCE_{38}-$CE_{40}CI_{22}$, and samples can be classified as calclithites and hybrid arenites (Fig. 5A). Concerning the siliciclastic content, the lack of feldspar and plutonic fragments discriminates this area (Fig. 5B, C), with a mean of $Q_{50}F_0L_{50}$. The sedimentary lithic fraction consists of quartz-rich sandstone and siltstone fragments and hybrid sandstones and siltstones. Metamorphic schist and phyllite fragments also occur in minor proportions. Samples from the Tremp syncline show higher amounts of lithic and carbonate extrabasinal grains than those from the Àger syncline (Fig. 5C) and also no clear vertical trends can be distinguished. All of these compositional characteristics indicate that samples from the Tremp syncline (Montrebei and Tremp sections) can be classified as "Carbonatic extrabasinal enriched" petrofacies (Fig. 5).

4.4.3. Vallcebre syncline and Cadí area

Samples from the Coll de Pal section (Cadí area) show a clear predominance of non-carbonatic extrabasinal grains, with high contents of quartz, feldspar (orthoclase) and granitoid fragments (Fig. 5D). Lithic grains, such as quartzarenites, metamorphic quartzites and schists and phyllites, are also present. The mean for this sector is $Q_{64}F_{18}L_{18}$, and samples can be classified as subarkoses and sublithoarenites (Fig. 5B). Because of the lack of carbonatic grains, samples from the Cadí monocline correspond to "siliciclastic dominant" petrofacies, which is restricted to this area.

In the Vallcebre area, most samples show dominance of non-carbonatic extrabasinal grains over the carbonatic grains (Fig. 5A). Concerning the quartz/feldspar/lithics content (Fig. 5B), these samples can be classified as "lithoarenites" (Pettijohn et al., 1972). Quartz and non-altered K-feldspar (orthoclase) are widely represented, with a plagioclase to K-feldspar ratio (P/K) that is less than 1. Carbonate extrabasinal grains are bioclastic micritic and wackestone-grainstone fragments. Intrabasinal components are coated grains and caliche nodules. All of the samples with these compositional characteristics can be associated with the "Mixed siliciclastic and carbonatic extrabasinal" petrofacies and are plotted in the same field area of the Àger syncline samples (Fig. 5C). Some layers show a clear predominance of carbonatic grains, represented mainly by a wide variety of Cretaceous limestones and recycled single orbitolinid grains, so an additional "Carbonatic extrabasinal enriched" petrofacies is also found in the Vallcebre syncline (Fig. 5A).

5. Implications and discussion

5.1. Provenance of detrital grains

The integration of petrology with regional geology is crucial for discussing the paleogeography of the Tremp Formation (Figs. 6 and 7). Thus, a first point to consider is the features of the detrital grains of the Tremp Formation that are informative regarding provenance.

Quartz origins in the Tremp Formation may be diverse because it appears in a wide range of varieties. Well-rounded quartz can be attributed to long distance transport or recycling from terrigenous grains from older sandstone formations. The presence of inherited quartz overgrowths in detrital quartz grains represents the cementation of grains from a previous sedimentary cycle (Sanderson, 1984). This type of detrital quartz suggests recycling of Paleozoic (Carboniferous or Permian formations) or Cretaceous formations. Fine-grained polycrystalline quartz can be associated with medium grade metamorphic rocks, such as schists and quartzites from the Paleozoic basement. Some euhedral quartz grains with evaporitic inclusions (halite and anhydrite) are similar to those described from the Triassic Keuper facies (Marfil, 1970). K-feldspar is attributed to crystalline rocks from the Paleozoic basement, such as granitoids or metamorphic units. Lithic grains, such as shales, schists, plutonic and radiolarite fragments, are also indicative of a contribution from the Paleozoic basement. Quartz-rich sandstones and siltstones can be attributed to Triassic Buntsandstein facies or Carboniferous formations, whereas hybrid sandstone and siltstone rock fragments are interpreted mainly as being supplied from the erosion of Mesozoic formations (characterised by the presence of carbonatic extrabasinal and intrabasinal components).

The provenance of carbonatic extrabasinal grains can be easily attributed to Mesozoic rocks. Mudstone and dolostone rock fragments can be interpreted as sourced from Triassic and Jurassic formations, whereas bioclastic limestone fragments are associated with contributions from Cretaceous formations. Some foraminifera contained in terrigenous grains validate the attribution of a Cretaceous age to these bioclastic limestone fragments. Moreover, wackestone fragments with pithonellid tests indicate a provenance of Upper Cretaceous limestones, whereas the occurrence of single orbitolines can be attributed to erosion from Lower Cretaceous formations.

Intrabasinal grains, such as oncolites and caliche nodules, are consistent with those described for the fluvial environments of the Tremp Formation (Colombo & Cuevas, 1993) indicating reworking of fluvial deposits and interstratified soils.

5.2. Paleogeographic implications

Paleogeographic reconstruction of the environmental settings of the Tremp Formation has been performed for the four stages between the Lower Maastrichtian to the Paleocene (Figs. 6 and 7). The location and the nature of source rocks is also established according to the three main defined petrofacies and provenance interpretations of the detrital grains.

5.2.1. Àger syncline

The Maastrichtian fluvial systems of the Àger basin are far more coarse-grained than those of the Tremp basin and have paleocurrents toward the north and northwest (Colombo & Cuevas, 1993; Cuevas, Dreyer, & Mercadé, 1989).

According to the grain provenance established, the "Mixed siliciclastic and carbonatic extrabasinal" petrofacies described for the Àger syncline sandstones is indicative of a contribution from source areas constituted by a Paleozoic basement and a Mesozoic carbonate cover. Siliciclastic grains, such as plutonic and low-grade metamorphic fragments, indicate contribution from Paleozoic source, whereas distinctive, reworked, euhedral quartz with evaporitic inclusions is attributed to Triassic Keuper facies. Carbonate extrabasinal grains, such as mudstones, dolostones and recycled Upper Cretaceous limestones, provide further evidence for the erosion of a Mesozoic cover.

Paleocurrents (Colombo & Cuevas, 1993; Cuevas et al., 1989) and facies distribution (Fig. 6) indicate sediment input from a southern area, whereas petrological data reveal a source area from Paleozoic basement and Mesozoic cover. The emergent zone acting as the southern basin margin during the Cretaceous has been defined as the Ebro Massif (Misch, 1934; Ziegler, 1990). Published data from subsurface exploration wells (Lanaja, 1987) demonstrates that the pre-Tertiary emergent basement in the Prades area (Fig. 1) was made of a thin Mesozoic cover and crystalline Paleozoic rocks. Additionally, results of thermal modelling from detrital apatite fission tracks (Juez-Larré & Andriessen, 2006) performed in the northern Prades block show that it remained above the apatite partial annealing zone during most of the Mesozoic, indicating that basement rocks of these areas were near the surface forming an elevated zone. Thus, we infer that the present-day Prades area, belonging to the Ebro Massif, acted as the source area for the Tremp Formation in the Àger syncline.

The southern provenance area for the Àger basin sandstones is inconsistent with the interpretations of Rosell et al. (2001) and

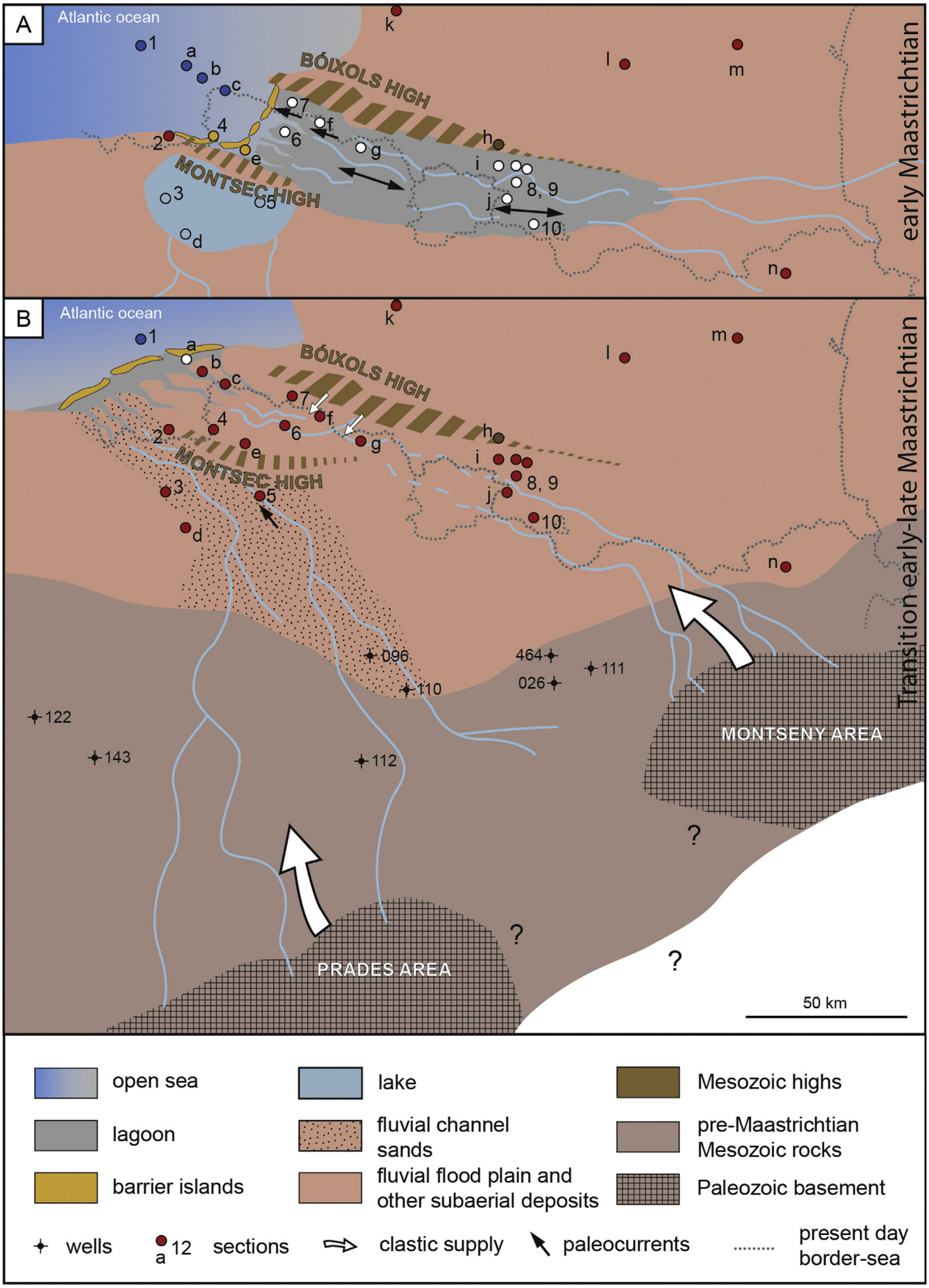

Fig. 6. Tectonically restored palaeogeographic reconstruction of the Tremp Formation during (A) the early Maastrichtian (lagoonal setting represented by the 'Grey Garumnian'; and during (B) the late Maastrichtian (fluvial-coastal setting represented by the 'Lower Red Garumnian'. Numbers represent the studied sections (see Fig. 1). Alphabetic characters represent areas or sections in which the paleoenvironment has been studied or work is in progress. a: Serraduy (López-Martínez et al., 2001); b: Iscles (López-Martínez et al., 2001; Vila et al., 2013); c: Areny (López-Martínez et al., 2001; Oms & Canudo, 2004; Pereda-Suberbiola et al., 2009); d: Embassament de Santa Anna; e–f: Terradets and Isona, respectively (Oms et al., 2015); g: Coll de Nargó (Riera, Anadón, Oms, Estrada, & Maestro, 2013); h: Pedraforca i: northern Vallcebre sector (Oms et al., 2015); j: Peguera (Vila et al., 2011); k: Le Mas d'Azil (Bilotte, Tambareau, & Villatte, 1983); l: Espéraza (Fondevilla et al., 2015); m: Albas (Galbrun, 1997); n: Boadella o: Montseny.

Ullastre and Masriera (1982). The latter authors considered an eastern origin because of the occurrence of kyanite, interpreted as being from the Sardinia and the Corsica Massifs. Kyanite has also been found in Oligocene rocks from the Ebro basin that were sourced from the southern Catalan Coastal Ranges as described in Allen and Mange-Rajetzky (1982). According to these authors,

Please cite this article in press as: Gómez-Gras, D., et al., Provenance constraints on the Tremp Formation paleogeography (southern Pyrenees): Ebro Massif *VS* Pyrenees sources, Cretaceous Research (2015), http://dx.doi.org/10.1016/j.cretres.2015.09.010

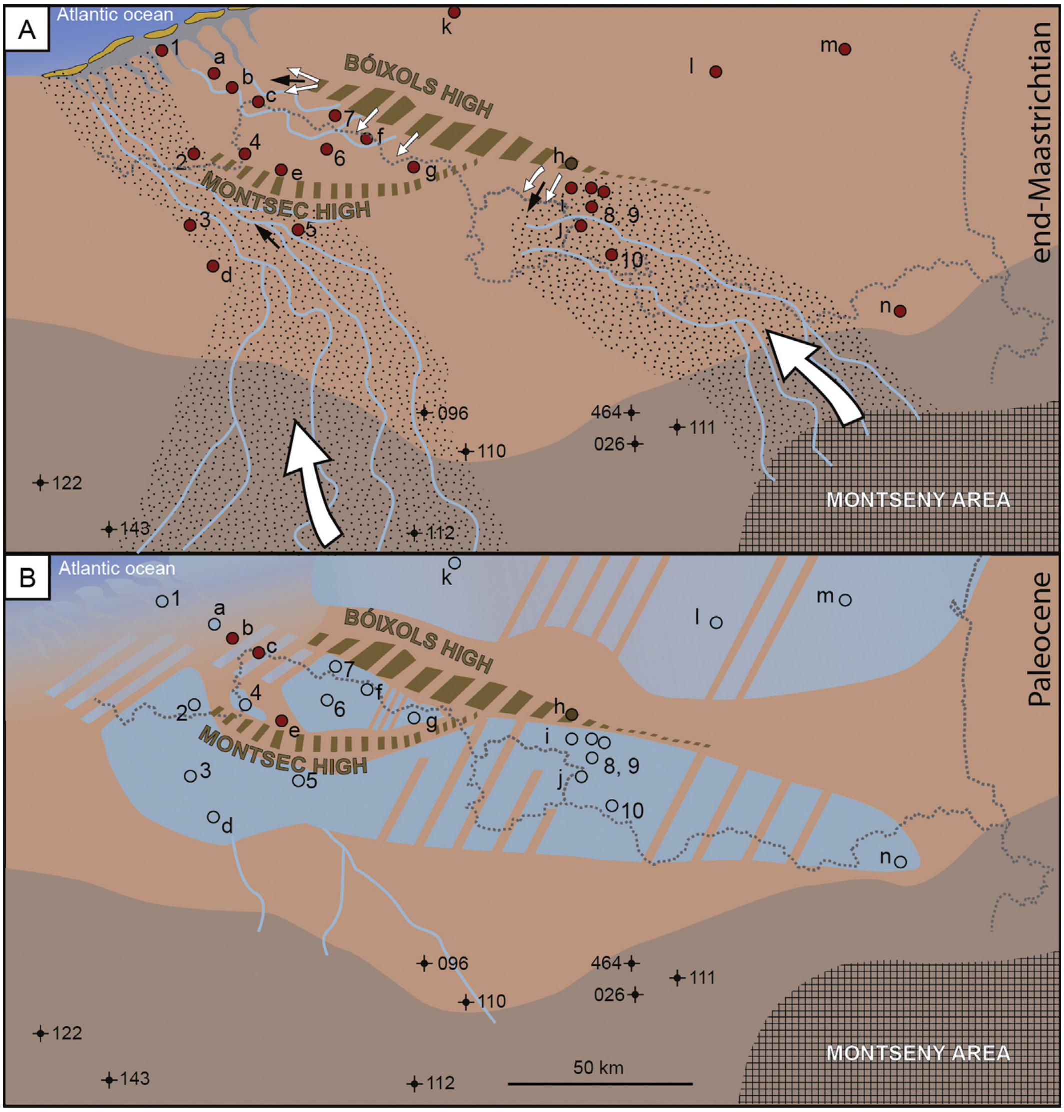

Fig. 7. Tectonically restored palaeogeographic reconstruction of the Tremp Formation during (A) latest-Maastrichtian (fluvial-coastal setting represented by the 'Lower Red Garumnian') and (B) early Paleocene (lacustrine setting represented by the 'Vallcebre limestone and laterally equivalent strata'). See legend in Fig. 6.

kyanite is distinctive from the Montsant area (south-western Catalan Coastal Ranges) and has not been reported in the Pyrenean derived sediments or in the Pyrenean basement. Kyanite has also been found in the Albian Escucha Formation that crops out in the Iberian Ranges (Sáinz-Amor, Cervera, Pardo, & Querol, 1996). Thus, the occurrence of kyanite in the Tremp Formation is not a diagnostic criterion for inferring an eastern source.

5.2.2. *Tremp and Coll de Nargó synclines*

The Tremp and Coll de Nargó synclines infill is dominated by the "Carbonatic extrabasinal enriched" petrofacies. The source area of these deposits is exclusively Cretaceous limestones (mainly Late Cretaceous) and a few sandstones. These compositions are also found in the Maastrichtian conglomerate and breccia deposits of the Tremp Formation attached to the Bóixols-Sant Corneli thrusts. In the Tremp syncline, these deposits are known as the Talarn and the Abella conglomerates (Krauss, 1990) and the Sallent de Montanisell-Coll de Nargó conglomerates (Rosell et al., 2001).

In the early and early-late Maastrichtian transition, paleocurrents were westward for the Areny Formation, 'Grey Garumnian' and the 'Lower Red Garumnian' (Cuevas, 1989 page 59; Díaz-Molina, 1987 pages 77,79,84). General westward and southwestward clastic progradation derived from Mesozoic highs has also been reported for the Tremp Formation by Eichenseer (1988). Paleocurrents in the Talarn conglomerates (late Maastrichtian) are toward the W and the WSW (Cuevas et al., 1987).

The sandstone composition is markedly different from that in the Àger basin because there are no fragments of crystalline basement (K feldspar and plutonic fragments). Undoubtedly, the source areas for the Tremp basin resulted from the erosion of the Sant Corneli anticline during the Maastrichtian as recorded by large sintectonic erosions (Deramond et al., 1993; Díaz-Molina, 1987) that are absent in the southern limb of the Montsec anticline. According to these distinct provenance signatures, the Tremp basin became isolated from the Àger basin because of the early growth of the Montsec anticline, preventing sediments derived from the Ebro Massif to reach the Tremp syncline (Fig. 7). The Tremp formation in the Benabarre area (Fig. 6) was deposited in the southern limb of the Montsec anticline. Despite that this area structurally belongs to the Montsec thrust unit, it was connected to the Àger basin and thus was fed by sediments derived from the Ebro Massif (i.e., the Benabarre area was to the south of the drainage divide resulting from the Montsec anticline).

5.2.3. Vallcebre syncline and Cadí area

The "Siliciclastic dominant" petrofacies is the only petrofacies found in the Cadí thrust sheet, whereas in the Vallcebre syncline, both "Carbonatic extrabasinal enriched" and "Mixed siliciclastic and carbonatic extrabasinal" petrofacies are found.

"Carbonatic extrabasinal enriched" from the Vallcebre syncline (Lower Pedraforca thrust sheet) displays a lot of Early and Late Cretaceous recycled orbitolinid grains and Late Cretaceous limestone fragments. These marine Cretaceous limestone fragments are the main component in the Coll de la Trapa conglomerates (Martínez, Berástegui, Losantos, & Schöllhorn, 2001). These conglomerates crop out stratigraphically below the Vallcebre limestone (i.e., they belong to the 'Lower Red Garumnian') and are derived from the early erosion of the Upper Pedraforca thrust sheet (Fig. 7) as shown by paleocurrents toward the SW (also described by Aepler (1967)).

As in the Àger syncline, "Mixed siliciclastic and carbonatic extrabasinal" petrofacies are also represented in the Vallcebre syncline. Thus, a source area composed of a Paleozoic basement and a Mesozoic cover is also established.

The "Siliciclastic dominant" petrofacies described in the Cadí area are characterised by lot of plutonic rock fragments, K-feldspar, quartz grains and metamorphic fragments that indicate erosion of a crystalline basement with no sedimentary cover.

A south-eastern source area can be inferred for the entire Cadí area and Vallcebre syncline. This is indicated by paleocurrents (Aepler, 1967) and that the entire succession in the Cadí area is coarser than in the Vallcebre syncline (Fig. 7). It must be considered that the Cadí unit (where proximal fluvial facies are found) was originally to the South of the Pedraforca unit (Vergés & Martínez, 1988).

Therefore, the Paleozoic source area for the Cadí and Vallcebre syncline must be toward the southeast in the Ebro Massif. We interpret that the most likely area of the Ebro Massif that could have fed these basins was the Montseny area. This is also supported by the lack of Mesozoic cover under Tertiary strata that lay directly on the crystalline basement (Puig-reig well), indicating exposure of Paleozoic rocks before Tertiary sedimentation. Thermal modelling from detrital apatite fission tracks (Juez-Larré & Andriessen, 2006) in the Montseny area show that the Paleozoic basement remained near the surface, forming an emergent zone from the Permian to the Tertiary. Further evidence of the Paleozoic rock exposures in this sector is also reported by Núñez, Gómez-Gras, and Maestro (2000) and Gómez-Gras, Lacasa, Núñez, and Sanfeliu (2000), who demonstrated that the Ebro Massif in the Montseny area was free from the Mesozoic cover because of non-sedimentation (see Figs. 6 and 7).

Additionally, the Vallcebre syncline records the supply of the early erosion of the Pedraforca thrust-sheet, providing all of the carbonatic grains found in both "Carbonatic extrabasinal enriched" and "Mixed siliciclastic and carbonatic extrabasinal" petrofacies. Nevertheless, the possible existence of a thin Mesozoic cover in the Ebro Massif, northwards to the Montseny area (Boadella area), could have contributed to the supply of carbonatic grains.

5.3. General considerations

In summary, the role of the Ebro Massif as the main source area during the Cretaceous can be unambiguously established because of its clear footprint in the Vallcebre-Cadí and Àger basins. This is also supported by previous paleogeographic reconstructions that report an exposed zone (Ebro Massif) in the north-eastern part of Iberia. The main sectors established in this work that constituted the Ebro Massif (Prades and Montseny area) are consistent with these paleogeographic reconstructions, main paleocurrents and well data. Additionally, thermal modelling performed in the Catalan Coastal Ranges (Prades and Montseny area) supports that these sectors were near the surface forming an elevated zone (Juez-Larré & Andriessen, 2006). Additionally, in the Ebro Massif, crystalline rocks underwent intense weathering because of long exposure from the Triassic to the Cretaceous (Gómez-Gras, 1993; Gómez-Gras & Ferrer, 1999; Gómez-Gras, Núñez, Lacasa, & Parcerisa, 2004; Parcerisa, Gómez-Gras, & Martín-Martín, 2007). This intense weathering is supported by the low P/K ratios found in all the samples from the Vallcebre and Àger synclines.

Concerning the northern source areas, they are restricted to Cretaceous cover thrust or thrust anticlines (Lower Pedraforca and Bóixols-Sant Corneli). Major basement exhumation took place later, during Eocene times (Barsó & Ramos, 2007; Beamud et al., 2011; Fitzgerald, Muñoz, Coney, & Baldwin, 1999). The occurrence of two main source areas (Pyrenees and Ebro Massif) for the south Pyrenean basin during the Late Cretaceous has important implications for understanding the geotectonic setting. For studies dating the Pyrenees exhumation, using detrital low temperature thermochronology is mandatory for a good control of the sediment provenance to determine which source area supplies the detrital grains. Thus, recent studies using detrital thermochronology to unravel the exhumational history of the Pyrenees should be revisited (for instance Whitchurch et al., 2011) because these authors considered zircons to be derived from the north, without considering the role of the Ebro Massif as a source area.

6. Conclusions

Petrofacies and sediment routing permit an accurate reconstruction of the paleogeography and the evolution of the late Cretaceous South Pyrenean foreland basin. Three main petrofacies can be identified: "Carbonatic extrabasinal enriched", "Siliciclastic dominant" and "Mixed siliciclastic and carbonatic extrabasinal". The first one would be mainly derived from the Pyrenean cover thrusts, while the second and third ones would be derived from the Ebro Massif.

The Àger and Vallcebre syncline sandstones were always sourced from areas consisting of a Paleozoic basement and a Mesozoic carbonate cover, interpreted as being in the Ebro Massif (located to the south). In the Vallcebre syncline, the supply of carbonate grains is derived from the early erosion of the Pedraforca thrust sheet. By contrast, in the Tremp syncline, these sandstones lacked the Paleozoic basement signal, indicating a main contribution from the Mesozoic cover derived from the erosion of the Bóixols-Sant Corneli anticline.

A south and southeast source area (Ebro Massif) is also supported by the fluvial features of the Tremp Formation, being coarser in the southern exposure areas (Àger basin and Cadí area). The south and southeast derived clasts only reached the northern edge of the south Pyrenean basin in the present-day Vallcebre syncline. By contrast, the early growth of the Montsec anticline topographic high prevented southern derived sediments from going further north.

In conclusion, the Àger basin was fed from the south (Prades area) and the Cadí-Vallcebre area was fed from the southeast (Montseny area), both areas belonging to the Ebro Massif. The Pyrenean basement (Axial Zone) was not a source area during the sedimentation of the Tremp Formation. This last point is in conflict with interpretations dating Pyrenean exhumation on the basis of detrital thermochronology without provenance determinations. The only source areas to the north of the south Pyrenean basin were the topographic highs resulting from cover thrusts. These provided marine Cretaceous marine rock fragments (both as sandstones and conglomerate deposits) that coexisted with the preeminent southern source area.

The complex foreland evolution of the south Pyrenean basin can now be better constrained involving early basin partitioning. Therefore, the Tremp, the Àger and the Vallcebre subbasins are integrated in a broken foreland basin scheme. The Tremp basin became isolated from the rest of the south Pyrenean basin because of the growth of the Montsec thrust. This isolation prevented sediments derived from the Ebro Massif from reaching the Tremp syncline, consistent with sedimentological data.

A time and space detailed picture for south Pyrenean basin evolution is summarised in four palaeogeographic diagrams representing the Maastrichtian and the transition to the Paleocene, contributing to the better understanding of a key area for the terrestrial End Cretaceous record.

Acknowledgements

This paper is a contribution to the projects CGL2011-30069-C02-02/BTE and CGL2014-54180-P, financed by the Ministerio de Economía y Competitividad of Spain. V. Fondevilla acknowledges support from the Ministerio de Economía y Competitividad, (FPI grant, BES-2012-052366). M. Roigé and S. Boya acknowledge support from the Universitat Autònoma de Barcelona (PIF grant). The reviewers and the editor (Dr. Eduardo Koutsoukos) provided useful comments to improve the manuscript. We would like to thank Conwy Valley Systems Limited to provide us PETROG™ software for the compositional data adquisition.

References

Aepler, R. (1967). *Das garumnian der Mulde Von Vallcebre und ihre Tektonik (Spanien, Provinz Barcelona)*. Master thesis (p. 101). Berlin: Freien Universität Berlin (Naturwissenschaftlichen Fakultät). Unpublished.

Allen, P., & Mange-Rajetzky, M. (1982). Sediment dispersal and palaeohydraulics of Oligocene rivers in the eastern Ebro Basin. *Sedimentology, 29*(5), 705–716.

Ardévol, L., Klimowitz, J., Malagón, J., & Nagtegaal, P. J. C. (2000). Depositional sequence reponse to foreland deformation in the Upper Cretaceous of the southern Pyrenees, Spain. *American Association of Petroleum Geologists Bulletin, 84*(4), 566–587.

Ashauer, H., & Teichmüller, R. (1935). Die variscische und alpidische Gebirgs bildung Kataloniens. Abhandlungen der Gesellschaft der Wissenschaften zu Göttingen. *Mathematisch-Physikalische, 16*, 16–98.

Barsó, D., & Ramos, E. (2007). Procedencia de los conglomerados sinorogénicos de La Pobla de Segur, Pirineos centro-meridionales. *Revista de la Sociedad Geológica de España, 41*, 19–22.

Beamud, E., Muñoz, J. A., Fitgerald, P. G., Baldwin, S., Garcés, M., Cabrera, L., et al. (2011). Magnetostratigraphy and detrital apatite fission track thermochronology in syntectonic conglomerates: constraints on the exhumation of the South-Central Pyrenees. *Basin Research, 23*(3), 309–331.

Beard, D. C., & Weyl, P. K. (1973). Influence of texture on porosity and permeability of unconsolidated sand. *American Association of Petroleum Geologists Bulletin, 57*, 349–369.

Bilotte, M., Tambareau, Y., & Villatte, J. (1983). Le Crétacé supérieur et la limite Crétacé-Tertiaire en faciès continental dans le versant nord des Pyrénées. *Géologie Méditerranéenne, 10*(3–4), 269–276.

Canudo, J. I., Oms, O., Vila, B., Galobart, À., Fondevilla, V., Puértolas-Pascual, E., et al. (2015). The late Maastrichtian dinosaur fossil record from the southern Pyrenees and its contribution to the topic of the Cretaceous-Palaeogene mass extinction event. *Cretaceous Research*. http://dx.doi.org/10.1016/j.cretres.2015.06.013.

Chayes, F. (1952). The finer-grained calcalkaline granites of New England. *Journal of Geology, 60*, 207–254.

Colombo, F., & Cuevas, J. L. (1993). Características estratigráficas y sedimentológicas del 'Garumniense' en el sector de Ager (Pre-Pirineo, Lleida). *Acta Geologica Hispanica, 28*(4), 15–32.

Combes, P. J. (1969). *Recherches sur la genése des bauxites dans le Nord-Est de l'Espagne, Le Languedoc et L'Ariége (France)*. PhD thesis (p. 275). Montpellier: Univ. Montpellier, Mém. Centre d'Etudes et Rech. Geol. et Hydroéol.

Costa, E., Garcés, M., López-Blanco, M., Beamund, E., Gómez-Paccard, M., & Cruz-Larrasoaña, J. (2010). Closing and continentalization of the South Pyrenean foreland basin (NE Spain): magnetochronological constraints. *Basin Research, 22*, 904–917.

Cuevas, J. L. (1989). *La Formación Talarn: Estudio estratigráfico y sedimentológico de las facies de un sistema aluvial en el tránsito Mesozoic-Cenozoico de la Conca de Tremp*. MsC thesis (p. 107). Universitat de Barcelona. Unpublished.

Cuevas, J. L. (1992). Estratigrafía del "Garumniense" de la Conca de Tremp. Prepirineo de Lérida. *Acta Geológica Hispánica, 27*(1–2), 95–108.

Cuevas, J. L., Dreyer, T., & Mercadé, R. (1989). The Tremp Group. Alluvial deposits of the successive foreland basin stages and their relation to the Pyrenean thrust sequences. In M. Marzo, & C. Puigdefàbregas (Eds.), *4th International Conference on Fluvial Sedimentology* (pp. 95–111). Publicacions del Servei Geològic de Catalunya.

Deramond, J., Souquet, P., Fondecave-Wallez, M. J., & Specht, M. (1993). Relationships between thrust tectonics and sequence stratigraphy surfaces in foredeeps: Model and examples from the Pyrenees (Cretaceous-Eocene, France, Spain). In *Geological Society, London, Special Publications 71(1)* (pp. 193–219).

Díaz-Molina, M. (1987). Sedimentación sintectónica asociada a una subida relativa del nivel del mar durante el Cretácico superior (Fm. Tremp, província de Lérida). In *Estudios Geológicos, volumen extraordinário Galve-Tremp* (pp. 69–93).

Dickinson, W. (1970). Interpreting detrital modes of graywacke and arkose. *Journal of Sedimentary Petrology, 40*, 695–707.

Dickinson, W. R., Beard, L. S., Breankenridge, J. L., Erjavec, R. C., Ferguson, K. F., Inman, R. A., et al. (1983). Provenance of North American Phanerozoic sandstones in relation to tectonic setting. *Geological Society of American Bulletin, 94*, 222–235.

Díez-Canseco, D., Arz, J. A., Benito, M. I., Díaz-Molina, M., & Arenillas, I. (2014). Tidal influence in redbeds: A palaeoenvironmental and biochronostratigraphic reconstruction of the Lower Tremp Formation (South-Central Pyrenees, Spain) around the Cretaceous/Paleogene boundary. *Sedimentary Geology, 312*, 31–49.

Dryden, A. L., Jr. (1931). Accuracy in percentage representation of heavy mineral frequencies. *Proceedings of the National Academy of Sciences of the United States of America, 17*(5), 233.

Dunham, R. J. (1962). Classification of carbonate rocks according to depositional texture. In W. E. Ham (Ed.), *Classification of carbonate rocks* (pp. 108–121). Tulsa, Okla: American Association of Petroleum Geologists.

Eichenseer, H. (1988). *Facies geology of late Maastrichtian to early Eocene coastal and shallow marine sediments (Tremp-Graus basin, Northeastern Spain)*. PhD thesis (p. 273). Tübingen University.

Feist, M., & Colombo, F. (1983). La limite Crétace-Tertiaire dans le nord-est de l'Espagne, du point de vue des Charophyites. *Géologie Méditerranéenne, 10*, 303–326.

Fitzgerald, P. G., Muñoz, J. A., Coney, P. J., & Baldwin, S. L. (1999). Asymmetric exhumation across the Pyrenean orogen: implications for the tectonic evolution of a collisional orogen. *Earth and Planetary Science Letters, 173*(3), 157–170.

Fondevilla, V., Dinarès-Turell, J., Vila, B., Le Loeuff, J., Estrada, R., Oms, O., et al. (2015). Magnetostratigraphy of the Maastrichtian continental record in the Upper Aude Valley (northern Pyrenees, France): placing age constraints on the succession of dinosaur-bearing sites. *Cretaceous Research*. http://dx.doi.org/10.1016/j.cretres.2015.08.009.

Galbrun, B. (1997). Did the European dinosaurs disappear before the KT event? Magnetostratigraphic evidence. *Earth and Planetary Science Letters, 148*(3), 569–579.

Galbrun, B., Feist, M., Colombo, F., Rocchia, R., & Tambareau, Y. (1993). Magnetostratigraphy and biostratigraphy of Cretaceous-Tertiary continental deposits, Ager Basin, Province of Lerida, Spain. *Palaeogeography, Palaeoclimatology, Palaeoecology, 102*, 41–52.

Garrido-Mejias, A., & Rios, L. M. (1972). Síntesis gelógica del Secundario y Terciario entre los rios Cinca y Segre. *Boletín Geológico y Minero de España, 83*(1), 1–47.

Garzanti, E., & Vezzoli, G. (2003). A classification of metamorphic grains in sands based on their composition and grade: Research Methods Papers. *Journal of Sedimentary Research, 73*(5), 830–837.

Gazzi, P. (1966). Le arenarie del flysh sopra cretaceo dell'Apenino modenese; correlazioni con il flysh Monghidoro. *Mineralogica et Petrographica Acta, 12*, 69–97.

Gazzi, P., Zuffa, G. G., Gandolfi, G., & Paganelli, L. (1973). Provenienza e dispersione litoranea delle sabbie delle spiagge adriatiche fra le foci dell'Isonzo e del Foglia: inquadramento regionale. *Memorie della Società Geologica Italiana, 12*, 1–37.

Gómez-Gras, D. (1993). El Permotrías de la Cordillera Costero Catalana: Facies y Petrología Sedimentaria. *Boletín Geológico y Minero, 104*(2), 115–161.

Gómez-Gras, D., & Ferrer, C. (1999). Caracterización petrológica de perfiles de meteorización antiguos desarrollados en granitos tardihercínicos de la Cordillera Costero Catalana. *Revista de la Sociedad Geológica de España, 12*(2), 281–299.

Gómez-Gras, D., Lacasa, G., Núñez, J. A., & Sanfeliu, T. (2000). Paleoperfiles de alteración en el sustrato granítico en el borde de la Cuencas Surpirenaica Oriental. *Geotemas, 2*, 103–106.

Gómez-Gras, D., Núñez, J. A., Lacasa, G., & Parcerisa, D. (2004). Provenance of the Eocene flood-related braid delta depositsfrom NE of Ebro basin (Spain). In *32nd International Geological Congress, Florència, Itàlia, Abstracts book 2* (p. 1099).

Graham, S. A., Tolson, R. B., Decelles, P. G., Ingersoll, R. V., Bargan, E., Caldwell, M., et al. (1986). Provenance modelling as a technique for analysing source terrane evoltuion and controls on foreland sedimentation. In *Special Publications of the International Association of Sedimentologists 8* (pp. 425–436).

Ingersoll, R. V., Bullard, T. F., Ford, R. L., Grimm, J. P., Pickle, J. D., & Sores, S. W. (1984). The effects of grain size on detrital modes: a test of the Gazzi-Dickinson point-counting method. *Journal of Sedimentary Petrology, 54*, 103–116.

Institut Geològic de Catalunya. (2010). Atles geològic de Catalunya. In *Generalitat de Catalunya. Barcelona* (p. 463).

Juez-Larré, J., & Andriessen, P. A. M. (2006). Tectonothermal evolution of the northeastern margin of Iberia since the break-up of Pangea to present, revealed by low-temperature fission-track and (U–Th)/He thermochronology: a case history of the Catalan Coastal Ranges. *Earth and Planetary Science Letters, 243*(1), 159–180.

Jurado, M. J. (1988). *El Triásico de la subcuenca del Ebro* (p. 327). Universidad de Barcelona. Ph. D. thesis.
Krauss, S. (1990). Stratigraphy and Facies of the "Garumnian"—Late Cretaceous to Early Paleogene—in the Tremp Region, Central Southern Pyrenees. In *Tübingen Geowis-senschaftliche Arbeiten. Reihe A. Nr. 11* (p. 152). Tübingen.
Lanaja, J. M. (1987). *Contribución de la exploración petrolífera al conocimiento de la geología de España*. Instituto Geológico y Minero de España.
Leymerie, A. (1862). Aperçu géognostique des Petites Pyrénées et particulièrement de la montagne d'Ausseing. *Bulletin de la Société Géologique de France, 19*, 1091–1096.
Liebau, A. (1973). El Maastrichtiense lagunar (Garumniense) de Isona. In *XIII Coloquio Europeo de Micropaleontología (Madrid, España)*.
Llopis, L. N. (1947). *Contribución al conocimiento de la morfoestructura de los Catalánides* (p. 372). Instituto Lucas Mallada.
López-Martínez, N., Canudo, J. I., Ardévol, L., Pereda-Suberbiola, X., Orue-Etxebarria, X., Cuenca-Bescós, G., et al. (2001). New dinosaur sites correlated with Upper Maastrichtian pelagic deposits in the Spanish Pyrenees: implications for the dinosaur extinction pattern in Europe. *Cretaceous Research, 22*, 41–61.
López-Martínez, N., Arribas, M. E., Robador, A., Vicens, E., & Ardèvol, L. (2006). Los carbonatos danienses (Unidad 3) de la Fm Temp (Pirineos sur-centrales): paleogeografía y relación con el límite Cretácico-Terciario. *Revista de la Sociedad Geológica de España, 19*(3), 233–255.
López-Martínez, N., Ardèvol, L., Arribas, M. E., Civis, J., & Gonzalez-Delgado, A. (1998). The geological record in non-marine environments around the K/T boundary (Tremp Formation, Spain). *Bulletin de la Société géologique de France, 169*(1), 11–20.
Mansfield, C. F. (1971). Stratigraphic variation in sandstone petrology of the Great Valley sequence in the Southern Coast Ranges west of Coalinga, California. In *GSA Abstracts with Programs (Cordilleran section) 3(2)* (p. 157).
Marfil, R. (1970). Estudio petrogenético del Keuper en el sector meridional de la Cordillera Ibérica. *Estudios Geológicos, 2*, 113–163.
Martínez, A., Berástegui, X., Losantos, M., & Schöllhorn, E. (2001). Estructura de los mantos superior e inferior del Pedraforca (Pirineos orientales). *Geogaceta, 30*, 183–186.
Mey, P. H. W., Nagtegaal, P. J. C., Roberti, K. J. A., & Hartelvelt, J. J. A. (1968). Lithostratigraphic sub-division of posthercynian deposits in the south central Pyrenees, Spain. *Leidse Geologische Mededelingen, 41*, 221–228.
Misch, P. (1934). Der Bau der Mitteleren Südpyrenäen. In *Abh. Gesellsch. Wissench. Göttingen, III. Folge, H. 12* (pp. 1–168).
Muñoz, J. A. (1992). Evolution of a continental collision belt: ECORS-Pyrenees crustal balanced section. In K. R. McClay (Ed.), *Thrust tectonics* (pp. 235–246). London: Chapman and Hall.
Nijman, W. (1989). Thrust sheet rotation?—The South Pyrenean Tertiary basin configuration reconsidered. *Geodinamica Acta, 3*, 17–42.
Núñez, J. A., Gómez-Gras, D., & Maestro, E. (2000). Petrología del Eoceno Inferior-Medio del borde S de la cuenca Surpirenaica Oriental. *Geotemas, 2*, 157–160.
Ogg, J. G., & Hinnov, L. A. (2012). Cretaceous. In F. M. Gradstein, & J. G. Ogg (Eds.), *The geologic time scale 2012* (Vol. 2, pp. 793–853). Elsevier.
Oms, O., & Canudo, J. I. (2004). Datación magnetoestratigráfica de los dinosaurios del Cretácico terminal (Maastrichtiense superior) de Arén (Huesca, Unidad Surpirenaica Central). *Geo-Temas, 6*(5), 51–54.
Oms, O., Dinarès-Turell, J., Vicens, E., Estrada, R., Vila, B., Galobart, À., et al. (2007). Integrated stratigraphy from the Vallcebre Basin (southeastern Pyrenees, Spain): new insights on the continental Cretaceous-Tertiary transition in southwest Europe. *Palaeogeography, Palaeoclimatology, Palaeoecology, 255*, 35–47.
Oms, O., Fondevilla, V., Riera, V., Marmi, J., Vicens, E., Estrada, R., et al. (2015). Transitional environments of the lower Maastrichtian South Pyrenean Basin (Catalonia, Spain): the Fumanya Member tidal flat. *Cretaceous Research*. http://dx.doi.org/10.1016/j.cretres.2015.09.004.
Oms, O., Vila, B., Marmi, J., Sellés, A. G., Galobart, À., Estrada, R., et al. (2014). Geological setting and environments of the Tremp Formation (Southeastern Pyrenees, Iberian Peninsula). Field trip guide. In *Paleontologia i Evololució Special memory 7* (pp. 1–50), ISBN 978-84-617-1336-3.
Parcerisa, D., Gómez-Gras, D., & Martín-Martín, J. D. (2007). Calcretes, oncolithes and lacustrine limestones in Upper Oligocene alluvial fans of the Montgat area (Catalan Coastal Ranges, Spain). In A. M. Alonso-Zarza, & L. Tanner (Eds.), *Special Paper GSA books, 416Paleoenvironmental record and applications of calcretes and palustrine carbonates* (pp. 105–118).
Pereda-Suberbiola, X., Canudo, J. I., Cruzado-Caballero, P., Barco, J. L., López-Martínez, N., Oms, O., et al. (2009). The last hadrosaurid dinosaurs of Europe: a new lambeosaurine from the uppermost Cretaceous of Arén (Huesca, Spain). *Comptes Rendus Palé, 8*(6), 559–572.
Pettijohn, F. J., Potter, P. E., & Siever, R. (1972). *Sand and sandstones* (p. 618). Berlin: Springer-Verlag.
Plaziat, J. C. (1981). Late Cretaceous to late Eocene paleogeographic evolution of southwest Europe. *Palaeogeography, Palaeoclimatology, Palaeoecology, 36*(3–4), 263–320.
Puigdefàbregas, C., Muñoz, J. A., & Vergés, J. (1992). Thrusting and foreland evolution in the Southern Pyrenees. In K. McClay (Ed.), *Thrust tectonics* (pp. 247–254). London: Chapman & Hall.
Pujalte, V., & Schmitz, B. (2005). Revision de la estratigrafía del Grupo Tremp ("Garumniense", Cuenca de Tremp-Graus, Pirineos meridionales). *Revista de la Sociedad Geológica de Espanya, 38*, 79–82.
Riera, V., Anadón, P., Oms, O., Estrada, R., & Maestro, E. (2013). Dinosaur eggshell isotope geochemistry as tools of palaeoenvironmental reconstruction for the upper Cretaceous from the Tremp Formation (Southern Pyrenees). *Sedimentary Geology, 294*, 356–370.
Riera, V., Oms, O., Gaete, R., & Galobart, À. (2009). The end-Cretaceous dinosaur succession in Europe: the Tremp Basin record (Spain). *Palaeogeography, Palaeoclimatology, Palaeoecology, 283*, 160–171.
Rosell, J. (1963). *Estudio geológico del sector del Pirineo comprendido entre los ríos Segre y Noguera Ribagorzana (prov. de Lérida)*. Tesis doctoral. Universidad de Barcelona. Publicada en Pirineos, nº 75–78, f. 9-214.
Rosell, J., Linares, R., & Llompart, C. (2001). El "Garumniense" Prepirenaico. *Revista de la Sociedad Geológica de España, 14*, 47–56.
Sáinz-Amor, E., Cervera, A., Pardo, G., & Querol, X. (1996). Mineralogía de los materiales detríticos de la Fm. Escucha (Albiense inferior) en el distrito minero de Teruel (sector Suroriental de la Cordillera Ibérica). *Acta Geológica Hispánica, 31*(4), 41–54.
Sanderson, D. (1984). Recognition and significance of inherited quartz overgrowths in quartz arenites. *Journal of Sedimentary Petrology, 54*(2), 473–486.
Simó, A. (1985). *Secuencias deposicionales del Cretácico superior de la Unidad del Montsec (Pirineo Central)*. PhD thesis (p. 325). Universitat de Barcelona.
Simó, A., & Puigdefabregas, C. (1985). Transition from shelf to basin on an active slope, upper Cretaceous, Tremp area, southern Pyrenees. In *Exc. Guide-book 6th European Regional Meeting. Lleida, Espanya* (pp. 63–108).
Souquet, P. (1967). *Le Crétacé supérieur sud-pyrénéen en Catalogne, Aragon et Navarre* (Thèses Sciences Toulouse, imp. PRIVAT, 529 p., 68 fig., 24 pl., 7 tabl., 1 carte).
Teixell, A., & Muñoz, J. A. (2000). Evolución tectonosedimentaria del Pirineo meridional durante el Terciario: una síntesis basada en la transversal del río Noguera Ribagorçana. *Revista de la Sociedad Geológica de España, 13*(2), 251–264.
Ullastre, J., & Masriera, A. (1982). Hipótesis y problemas acerca del origen de las Asociaciones de minerales pesados del Senoniense del Pirineo Catalán. *Cuadernos de Geología Ibérica, 8*, 949–964.
Van Hoorn, B. (1970). Sedimentology and Paleogeography of an Upper Cretaceous turbidite basin in the South-central Pyrennés. *Leids Geologisehe Medelingen, 45*, 73–154.
Van der Plas, L., & Tobi, A. C. (1965). A chart for judging the reliability of point counting results. *American Journal of Science, 263*(1), 87–90.
Vergés, J. (1999). Estudi geològic del vessant sud del Pirineu oriental i central. Evolució cinemàtica en 3D. In *Monografies tècniques, 7* (p. 192). Instiut cartogràfic de Catalunya.
Vergés, J., & Burbank, D. W. (1996). Eocene–Oligocene thrusting and basin configuration in the eastern and central Pyrenees (Spain). In P. F. Friend, & C. J. Dabrio (Eds.), *Tertiary basins of Spain* (pp. 120–133). Cambridge University Press.
Vergés, J., & Martínez, A. (1988). Corte compensado del Pirineo oriental: Geometría de las cuencas de antepaís y edades de emplazamiento de los mantos de corrimiento. *Acta Geológica Hispánica, 2*, 95–105.
Vicens, E., Ardèvol, L., López-Martínez, N., & Arribas, M. E. (2004). Rudist biostratigraphy in the Campanian-Maastrichtian of the south-central Pyrenees, Spain. In *Courier Forschung - Institut Senckenberg 247* (pp. 113–127).
Vicente, A., Martín-Closas, C., Arz, J. A., & Oms, O. (2015). Maastrichtian– basal Paleocene charophyte biozonation and its calibration to the Global Polarity Time Scale in the southern Pyrenees (Catalonia, Spain). *Cretaceous Research, 52*, 268–285.
Vila, B., Galobart, À., Canudo, J., Le Loeuff, J., Dinarès-Turell, J., Riera, V., et al. (2012). The diversity of sauropods and their first taxonomic succession from the latest Cretaceous of southwestern Europe: clues to demise and extinction. *Palaeogeography, Palaeoclimatology, Palaeoecology, 350–352*, 19–38. http://dx.doi.org/10.1016/j.palaeo.2012.06.008.
Vila, B., Oms, O., Fondevilla, V., Gaete, R., Galobart, À., Riera, V., et al. (2013). The latest succession of dinosaur tracksites in Europe: hadrosaur ichnology, track production and palaeoenvironments. *PLoS One, 8*(9), e72579. http://dx.doi.org/10.1371/journal.pone.0072579.
Vila, B., Riera, V., Bravo, A., Oms, O., Vicens, E., Estrada, R., et al. (2011). The chronology of dinosaur oospecies in south-western Europe: refinements from the Maastrichtian succession from the eastern Pyrenees. *Cretaceous Research, 32*, 378–386.
Villalba-Breva, S., & Martín-Closas, C. (2012). Upper Cretaceous paleogeography of the Central Southern Pyrenean Basins (Catalonia, Spain) from microfacies analysis and charophyte biostratigraphy. *Facies*. http://dx.doi.org/10.1007/s10347-012-0317-1.
Whitchurch, A., Carter, A., Sinclair, H., Duller, R. A., Whittaker, A. C., & Allen, P. A. (2011). Sediment Routing sysytem evolution within a diachronously uplifting orogen: insights from detrital zircon thermochronologicla analyses from the south-central Pyrenees. *American Journal of Science, 311*, 442–482.
Ziegler, P. A. (1990). *Geological atlas of western and Central Europe* (2nd ed., p. 239). Shell Intern. Petroleum Mij. B. V. and Geol. Soc. London.
Zuffa, G. (1980). Hybrid arenites: their composition and classification. *Journal of Sedimentary Petrology, 50*, 21–29.
Zuffa, G. (1985). In G. G. Zuffa (Ed.), *Optical analyses of arenites: Influence of methodology on compositional results* (pp. 165–189). Provenance of Arenites, Boston.

Appendix A. Supplementary data

Supplementary data related to this article can be found at http://dx.doi.org/10.1016/j.cretres.2015.09.010.